



**N OVA**  
NOVA SCHOOL OF  
SCIENCE & TECHNOLOGY

DEPARTMENT OF  
LIFE SCIENCES

MARIA GONÇALVES ALCAIDE  
BSc in Biochemistry

DRUG DISCOVERY FROM CNIDARIANS:  
DELIVERY, BIOREACTIVITY AND MOLECULAR  
CHARACTERISATION OF TOXINS FROM THE  
SEA ANEMONE *ACTINIA EQUINA*

MASTER IN MOLECULAR GENETICS AND BIOMEDICINE  
NOVA University Lisbon  
September, 2022





# DRUG DISCOVERY FROM CNIDARIANS: DELIVERY, BIOREACTIVITY AND MOLECULAR CHARACTERISATION OF TOXINS FROM THE SEA ANEMONE *ACTINIA EQUINA*

**MARIA GONÇALVES ALCAIDE**

BSc in Biochemistry

**Adviser:** Pedro Manuel Brôa Costa  
*Auxiliary Professor, NOVA University Lisbon*

**Co-advisers:** Mariaelena D'Ambrosio  
*Postdoctoral Researcher, NOVA University Lisbon*

**Examination Committee:**

**Chair:** Margarida Casal Ribeiro Castro Caldas Braga  
*Auxiliary Professor, NOVA University Lisbon*

**Rapporteur:** Ana Luísa Maulvault  
*Auxiliary Researcher, Instituto do Mar e da Atmosfera*

**Adviser:** Pedro Manuel Brôa Costa  
*Auxiliary Professor, NOVA University Lisbon*



**Drug Discovery from Cnidarians:**

**Delivery, Bioreactivity and Molecular Characterisation of Toxins from the Sea Anemone *Actinia***

Copyright © Maria Gonçalves Alcaide, NOVA School of Science and Technology, NOVA University Lisbon.

The NOVA School of Science and Technology and the NOVA University Lisbon have the right, perpetual and without geographical boundaries, to file and publish this dissertation through printed copies reproduced on paper or on digital form, or by any other means known or that may be invented, and to disseminate through scientific repositories and admit its copying and distribution for non-commercial, educational or research purposes, as long as credit is given to the author and editor.



## ACKNOWLEDGMENTS

I would like to start by thanking my advisers, Pedro Costa and Mariaelena D'Ambrosio, for their support throughout this past year. I had many questions, failures and doubts but none of those was left unattended. I am very grateful for the opportunity to have worked on this team and it is thanks to them that I achieved the quality of this work.

To the members of SeaTox Lab, Cátia, Carla, Carolina, Inês and Madalena, I would like to thank them for welcoming me to the team with such smiles and good energy. Working alongside them was a true pleasure.

I would also like to thank Bruno Manadas and Vera Mendes (CNC, U.Coimbra) for the LC-MS/MS analysis, Prof. António Pedro de Matos and Pedro Henriques (C.I.I.E.M.) for the help with TEM and SEM analysis and Leonor Saúde and Lara Carvalho (IMM, U. Lisboa) for the help and contribution in the zebrafish assays.

To my colleagues, Miguel and Mariana, I thank them for the journey we shared and for the partnership in keeping our little animals alive.

To my friends, for all the support they gave me this past year. All the laughs, crying sessions, but most of all the love I received from you was always appreciated. To 3<sup>o</sup>E, for all the memories. To my housemates, the love among the chaos that I will always cherish.

To Leonor and Raquel, I mostly thank them for keeping me sane in this last sprint to the finish line. They were incredible supporters, and I am incredibly thankful for them.

Lastly, but most importantly, to my family. Especially my parents who were the first to listen to my complaints or worries. I thank them for always supporting my decisions, good and bad, and for the unconditional love I received my whole life.

Thank you all, from the bottom of my heart.



“Time has come to make things right.” (MUSE).



## ABSTRACT

Marine biodiversity is an invaluable source of natural bioactives of great interest for drug discovery, with emphasis on toxins, due to their potential specificity. Cnidarians, in particular, are known to secrete toxins for predation and defence, most of which are not fully described yet. This study on the sea anemone *Actinia equina*, common in the intertidal zone of the Portuguese coast, is a contribution to the study of the venom-delivery system of the abundant green and red varieties with the ultimate aim of disclosing its biotechnological potential as a source of bioactive compounds. *Actinia equina*'s anatomy and microanatomy were evaluated through electron and optical microscopy. Proteomics based on LC-MS/MS screening was employed to characterise proteinaceous toxins in the tentacles. The toxicity of the extracts was assessed in dechorionated zebrafish embryos and the survival rate was observed in a total of 72 hours of exposure. Structural analyses of the sea anemone confirmed the presence of specialized venom-cells in the tentacles, the nematocysts, responsible for injecting the venom into the prey. Proteomics identified a total of 286 proteins, of which 68 were exclusive to red specimens and 102 to green, leaving 116 proteins in common. The three most representative Gene Ontology terms related to Biological Process were “proteolysis”, “hemolysis in another organism” and “lipid catabolic process”. Various actitoxins, including specific to *Actinia equina*, were identified and classified as secreted Type I sodium channel inhibitory toxins (neurotoxins). Extracts from either variety were able to cause toxicity to zebrafish embryos, however, the venom of green anemones was seemingly more potent. Dose-effect relationships were found for both types of venom, even though the extracts from green anemones produced a more rapid effect (24 vs. 48h, comparatively). Altogether, the findings did not only show that proteinaceous toxins are present in the sea anemone *Actinia equina*, but also that different varieties can bear distinct bioactives with different bioreactivity, which increases the span of compounds of interest from the species for biotechnological and biomedical purposes, including but not exclusive to anaesthetics and painkillers.

**Keywords:** Drug Discovery, Venom, Toxicity, Proteomics, *Actinia equina*, Marine invertebrates



## RESUMO

A biodiversidade marinha é uma fonte valiosa de compostos bioativos naturais de interesse para desenvolvimento de fármacos, com ênfase nas toxinas devido à sua potencial especificidade. Os cnidários, em particular, são conhecidos por secretar toxinas para predação e defesa, que na sua maioria ainda não estão totalmente descritas. O presente estudo acerca da anémone marinha *Actinia equina*, comum na zona intertidal da costa portuguesa, contribui para o estudo do sistema de entrega de veneno das variedades verde e vermelha, com o objetivo de revelar o seu potencial biotecnológico como fonte de compostos bioativos. A anatomia e microanatomia de *Actinia equina* foram estudadas através de microscopia ótica e eletrónica. Proteómica baseada em LC-MS/MS foi aplicada para a caracterização de toxinas proteicas presentes nos tentáculos. A toxicidade dos extratos foi avaliada em embriões de peixe-zebra descorionados e a taxa de sobrevivência foi observada num total de 72 horas de exposição. A análise estrutural da anémone confirmou a presença de células especializadas de veneno nos tentáculos, os nematocistos, responsáveis pela injeção de veneno na presa. A análise proteómica permitiu identificar um total de 286 proteínas, das quais 68 foram encontradas exclusivamente em espécimes vermelhos e 102 em verdes, restando 116 proteínas em comum. Os termos “Gene Ontology” mais representativos relacionados com Processo Biológico foram “proteólise”, “hemólise noutro organismo” e “processo catabólico lipídico”. Várias actitoxinas, incluindo específicas de *Actinia equina*, foram identificadas e classificadas como toxinas secretadas inibidoras de canais de sódio tipo I (neurotoxinas). Extratos de ambas as variedades foram capazes de induzir toxicidade nos embriões de peixe-zebra, contudo, o veneno de anémons verdes aparentou ser mais potente. Foram encontradas relações dose-efeito para ambos os tipos de veneno, ainda que os extratos de anémons verdes tenham produzido um efeito mais rápido (24 vs. 48h, comparativamente). No geral, as descobertas não só demonstraram que toxinas proteicas estão presentes na anémone *Actinia equina*, mas também que diferentes variedades podem conter bioativos distintos, com bioreatividade diferente, o que aumenta a amplitude de compostos de interesse desta espécie para fins biotecnológicos e biomédicos incluindo, por exemplo, anestésicos e analgésicos.

**Palavras chave:** Veneno, Toxicidade, Proteómica, *Actinia equina*, Invertebrados marinhos



# CONTENTS

<b>1. INTRODUCTION .....</b>	<b>1</b>
<b>2. MATERIALS AND METHODS .....</b>	<b>5</b>
2.1. Animal Collection.....	5
2.2. Microscopy Analyses .....	5
2.3. Toxicity Testing .....	6
2.4. Characterisation of the Venom Proteome.....	7
2.5. Statistical Analysis.....	8
<b>3. RESULTS .....</b>	<b>11</b>
3.1. Histological analysis of <i>Actinia</i> 's cnidocytes .....	11
3.2. Toxicity Testing.....	15
3.3. Characterisation of Venom Proteins .....	17
<b>4. DISCUSSION .....</b>	<b>23</b>
<b>5. CONCLUSION.....</b>	<b>27</b>
<b>REFERENCES.....</b>	<b>30</b>



## LIST OF FIGURES

Figure 1.1.- Common varieties of sea anemone <i>Actinia equina</i> .....	3
Figure 3.1- External structure of <i>Actinia equina</i> .....	11
Figure 3.2- Microanatomy of tentacles from green specimens of <i>Actinia equina</i> .....	12
Figure 3.3- The epidermis layer of a tentacle of a red specimen of <i>Actinia equina</i> .....	12
Figure 3.4- Differentially stained cnidae in the epidermis of tentacles of an <i>A.equina</i> .....	13
Figure 3.5- Cnidae in the epidermis layer of tentacles of <i>Actinia equina</i> .....	14
Figure 3.6- Microanatomy of the body wall of <i>Actinia equina</i> .....	15
Figure 3.7- SDS.PAGE of protein extracts of <i>Actinia equina</i> stained with Coomassie Blue (A) and Silver Nitrate (B).....	15
Figure 3.8- Zebrafish embryo toxicity testing of extracts from green and red <i>Actinia equina</i> .....	16
Figure 3.9- The effect of Total Protein Concentration ( $\mu\text{g}/\mu\text{L}$ ) over the Survival Count at 72h of Exposure .....	17
Figure 3.10- SDS-PAGE of protein extracts from <i>Actinia equina</i> stained with Coomassie Blue.....	17
Figure 3.11- The most abundant protein families identified in (A) green and (B) red samples. ....	20
Figure 3.12- The number of proteins associated with the most frequent Biological Process Gene Ontology (GO) terms of proteins exclusively identified in (A) green and (B) red specimens. ....	21



## **LIST OF TABLES**

Table 3.1- Examples of toxins commonly identified in green and red specimen extracts .....	18
Table 3.2- Examples of toxins exclusively identified in green specimen extract .....	18
Table 3.3- Examples of toxins exclusively identified in red specimen extract .....	19



## ACRONYMS

<b>DMSO</b>	Dimethyl sulfoxide
<b>DNA</b>	Deoxyribonucleic acid
<b>DPX</b>	Dibutylphthalate polystyrene xylene
<b>DTT</b>	Dithiothreitol
<b>FDA</b>	Food and Drug Administration
<b>GA</b>	Glutaraldehyde
<b>GO</b>	Gene Ontology
<b>LC-MS/MS</b>	Liquid chromatography coupled to tandem mass spectrometry
<b>MNPs</b>	Marine Natural Products
<b>PAS</b>	Periodic acid-Schiff's reagent
<b>PBS</b>	Phosphate buffer saline
<b>PFA</b>	Paraformaldehyde
<b>SDS</b>	Sodium dodecyl sulphate
<b>SDS-PAGE</b>	Sodium dodecyl sulphate-polyacrilamide gel eletrophoresis
<b>SEM</b>	Scanning electron microscopy
<b>TEM</b>	Transmission electron microscopy



# | 1. INTRODUCTION

Natural products and their derivatives have an important role in drug discovery, especially if they bear both high specificity and bioactivity, which makes toxins particularly interesting targets for bioprospecting. Notwithstanding, marine species, as they occupy the richest and most diverse habitat on the planet, have become a prime target for research due to their high biodiversity since the broad ranges of temperature, light, pressure and nutritional conditions surpass those on land (Lindequist, 2016). Additionally, in a National Cancer Institute (NCI) preclinical toxicity screening for anti-tumour properties, crude marine bioproducts of various origins showed higher incidence of significant bioactive properties when compared to extracts from terrestrial origin (Montaser & Luesch, 2011), including toxins which have evolved to interact with specific molecular targets, proving that these are an important source for the efficacy of natural drug discovery (Kong et al. 2010). A few marine-derived products have been successfully launched to the market, the most well-known being “Ziconotide”, commercialized as “Prialt”, the first pain-killer derived from a marine bioproduct to be approved by the Food and Drug Administration (FDA) of the USA. This drug is a synthetic form of an  $\omega$ -conotoxin, a toxin from the poisonous cone snail *Conus magus*, and is used for treating severe and chronic pain (Molinski, 2009; Lindequist, 2016; Williams et al., 2008). More recently, Trabectedin, a DNA-binding agent derived from the marine tunicate *Ecteinascidia turbinata*, commercialized as “Yondelis”, has been approved in Europe for the treatment of soft-tissue sarcoma and ovarian cancer (Christinat & Leyvraz, 2009).

Venomous organisms are one of the targets of research for bioactive elements since their venoms consist of a complex mixture of proteins, peptides and other compounds that have evolved to disturb the activity

of enzymes, ion channels, and receptors associated with vital systems of the prey, such as the nervous system, blood coagulation and homeostasis (Calvete et al., 2009).

Cnidaria, a phylum of marine invertebrates that includes, for example, sea anemones, corals and jellyfish, and is known to be one of the oldest lineages of venomous animals (Jouiaei et al. 2015), is of great interest in the search of new bioproducts and has provided knowledge on over 3000 marine natural products (Rocha et al., 2011). As soft-bodied animals, many of which sessile, they rely on their venoms for protection from predators and the capture of prey (Sher et al., 2005). The cnidarian venoms have not been completely described yet, but seem to contain various proteinaceous (peptides, enzymes, and proteinase inhibitors) and non-proteinaceous compounds (purines, betaines, and others) (see for instance the review by D'Ambra & Lauritano, 2020). Although there are no cnidarian-derived drugs approved yet, some compounds are already being subjected to clinical trials. For example, ShK, a potassium-channel toxin isolated from the venom of the sea anemone *Stichodactyla helianthus*, was the source for “Dalazatide” (previously known as ShK-186), a synthetic peptide that is a specific inhibitor of the voltage-gated Kv1.3 potassium channel and has been trialled for the treatment and management of autoimmune diseases such as psoriasis (Tarcha et al., 2017), rheumatoid arthritis (Beeton et al., 2005), obesity and insulin resistance (Upadhyay et al., 2013). Most of the identified toxins, mainly classified as sodium and potassium-channel binding neurotoxins and pore-forming cytolytins, are found in specialized poisonous cells called cnidocytes. These cells are mostly located in the tentacles but can also be found in the acrorhagi, aggressive organs lodged around the base of the tentacles acting as a defense mechanism for non-clonal anemones, and acontia, thin threads attached to the mouth or the body wall of the anemone for defense or capture of prey (Frazão et al., 2012). The cnidae (or cnidocysts), membrane-enclosed cellular organelles belonging to the cnidocytes, are the defining subcellular specialisation of the phylum Cnidaria (Jouiaei et al., 2015).

The sea anemone *Actinia equina* (Fig. 1) is a benthic cnidarian, very common on rocky shores. Belonging to the Anthozoa class, these anemones have no medusa stage in their life cycle (the planktonic freeliving

stage), existing only as polyps (the benthic stage), and although they are described as sessile, most sea anemones change positions through slow sliding movements, especially during aggressive encounters. *Actinia* is formed by a smooth column, typically red, green, or brown, with a blue line on the edge of the base. The tentacles are located on the oral disc, surrounding the mouth of the polyp. This species is found in depths of about 20 m and the intertidal zones, attached to rocks or substrates by the basal disc, making them resistant to high temperatures and desiccation (Fish & Fish, 2011).

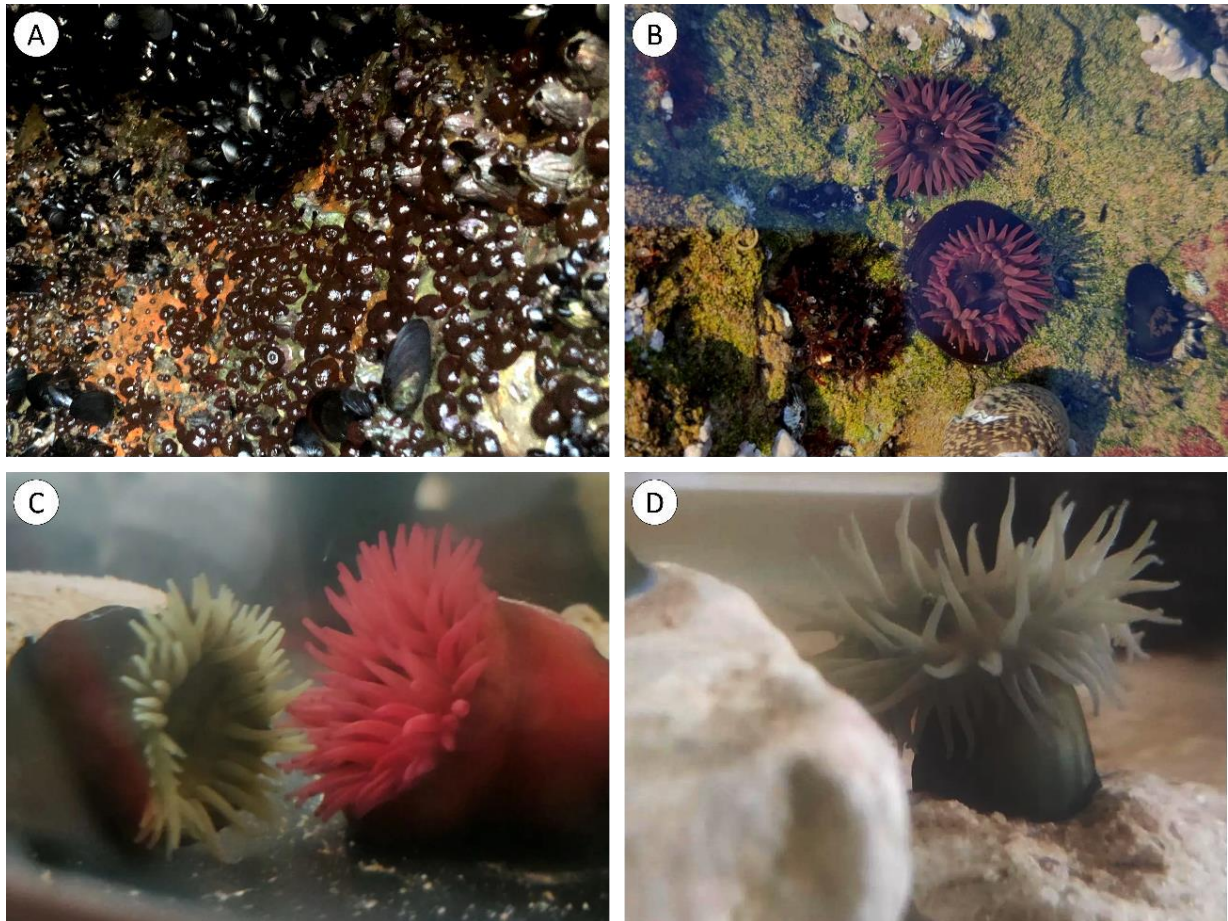


**Figure 1.1.- Common varieties of sea anemone *Actinia equina*** (A) Red specimens found in the intertidal zone of the shore in Costa da Caparica, Portugal, during low tide. (B) Red specimens found in an intertidal pool in Parede, Portugal. (C) Green and red specimens collected in Cabo Raso, Cascais, Portugal, (D) Green specimens collected in Costa Da Caparica, Portugal

In *Actinia equina*, the cnidae are classified as nematocysts, spined or un-spined thread that lacks hollow tubules or folds along their length (Mariscal, 1984). In the tentacles, where nematocysts are most abundant, these have spines along the full length of the tube (isorhizous holoritchs) and are used by the organisms mainly for the capture and envenomation of the prey and against predators by injecting the

venom (Turk & Kem, 2009), whereas the nematocysts present in the acrorhagi lack spines (atrichs) and are used in territorial defense, mainly against non-clonal conspecific anemones (Shick, 1991).

Previously, studies have intended to describe the composition of the venom of *Actinia equina*. The identified components, mostly proteinaceous, were classified as neurotoxins, cytolytins, and Kunitz-type peptides responsible for the paralysis, immobilization, and death of the prey (Menezes & Thakur, 2022). However, there are no studies regarding the possible variability of venom composition between different varieties of *Actinia*. Although this species is not harmful to humans, the identification of these components and their mechanisms of action can be beneficial to developing effective treatments for cnidarian envenomation since they can be similar to the ones present in other specimens of the phylum, as well as developing marine-derived drugs, biopesticides and molecular probes.

This work intends primarily to contribute to the study of the venom system of the sea anemone *Actinia equina* as a potential source of bioactive compounds with biotechnological potential for drug discovery. Specifically, this work aims to:

- i) Characterise the morphoanatomy of the venom-delivery apparatus;
- ii) Extract and identify the main proteinaceous toxins and associated potential bioactives present in the venom;
- iii) Evaluate venom bioreactivity/toxicity;
- iv) Compare the venom system between the two most common varieties of *Actinia equina*, “red” and “green”.

## MATERIALS AND METHODS

### 2.1. Animal Collection

Live *Actinia equina* were hand-collected during low tide, from the intertidal zone of the rocky shore in Cabo Raso, Cascais, Portugal (38°42'36.4"N 9°29'10.1"W) in October 2021, and from Costa da Caparica, Portugal (38°39'03.9"N 9°14'50.3"W) in February and April 2022. The animals were transported alive in seawater to the laboratory and kept in a closed circulation aquaria mesocosm fitted with constant aeration, water filtration and water recirculation. The water salinity, temperature, and photoperiod were controlled at about 30 ppt, 20 °C, and 16:8 h light:dark cycle, respectively. Animals were fed to the mouth twice a week with marine carnivore-pelleted food (Hikari). Animals were acclimatized for 7-14 days until processing and only two animals were lost during this period.

### 2.2. Microscopy Analyses

Tentacles from different *Actinia equina* were fixed with glutaraldehyde (GA) (2.5% v/v glutaraldehyde in 0.1M phosphate buffer saline (PBS), pH 7.4) for two hours at room temperature. Fixation was followed by washing with PBS (3 × 15 min), overnight post-fixation in 1% m/v osmium tetroxide (OsO<sub>4</sub>), 0.1 M PBS, pH 7.4 and washing in Milli-Q-grade ultrapure water (3 × 10 min). Three tentacles from each sample were selected and dehydrated in a progressive series of acetone (30%, 50%, 70%, 90% for 10 min each and 100% 3 × 10 min). Whole specimens, after being anaesthetized in ice-cold menthol for 15 min, were cut in half before embedding and positioned in the resin to permit transversal sectioning. Intermediate infiltration was done with EPON resin and polypropylene oxide (1:2, 1:1, and 2:1, for 30 min each) followed by a final infiltration with EPON resin (Sigma-Aldrich), in vacuum, for 30 min. The resin blocks were left to polymerize overnight at 50°C. Samples were cut into sections with 2µm thickness using a RM 2125 RTS rotatory microtome (Leica Microsystems) equipped with a tungsten carbide blade. Sections were stained using Toluidine Blue, Coomassie Blue and a tetrachromatic technique. The latter combines Alcian Blue for acidic mucins and sugars, Periodic acid-Schiff's (PAS) for sugars, Weigert's Hematoxylin and Picric Acid for muscle fibres and cytoplasm, respectively (Costa,

2018). The slides were mounted with DPX resin and observations were performed using a DM 2500 model microscope (Leica Microsystems).

Thin resin sections were analysed by transmission electron microscopy (TEM). This procedure was done in collaboration with *Centro de Investigação Interdisciplinar Egas Moniz* (CiiEM). Preparation of samples first involved collecting the thin sections produced with a Ultramicrotome Reichert-Jung Ultracut E, onto copper mesh grids and contrasting with 2% m/v aqueous Uranyl Acetate for 1 h and 20 min and Reynold's Lead Citrate for 8 min (Venable & Coggeshall, 1965). Observations were done using a JEOL 100- SX model TEM operated at 80 keV.

The external structure of the specimens was analysed by scanning electron microscopy (SEM). After fixation with glutaraldehyde (GA) (2.5% v/v glutaraldehyde, 0.1M PBS, pH 7.4), followed by post-fixation in 1% m/v osmium tetroxide (OsO<sub>4</sub>), 0.1 M PBS, pH 7.4, samples were dehydrated in a progressive series of acetone (30, 50%, 70%, 90% for 10 min each, and 100% 3 × 10 min). Then, samples were infiltrated with *tert*-butanol (3 × 15 min) at 40°C and left to freeze overnight at 4°C. The *tert*-butanol was sublimated under vacuum until samples were completely dry (Inoué & Osatake, 1988). The samples were mounted onto an aluminium plate with cooper ribbon for carbon coating using a JEOL JEE-400 vacuum evaporator. Analyses were performed in a JEOL JSM-5400 Scanning Microscope operated at 20 keV.

### **2.3. Toxicity Testing**

Three red and three green sea anemones ( $n=3$ ) were retrieved from the rearing system into separate Erlenmeyers, each pre-prepared with 10 drops of filtered and autoclaved seawater. The animals were let to rest for a few minutes while being mechanically stimulated to release their mucus. The sea anemones were then gently retrieved back to the rearing system and the mucus was transferred to a fresh microtube, where complemented buffer (Tris-HCl, pH 7.0 with 10% DTT and 1% protease inhibitor cocktail) was added in a 1:1 proportion. The samples were centrifuged for 5 min, 5000 rpm, at 4°C, and the supernatant was transferred to a fresh microtube, discarding the pelleted debris. The samples were first filtrated with a 0.22µm cellulose acetate syringe filter (FilterLab) and then filtrated using 100 kDa Amicon Ultra centrifugal filters (Merck). The filtrate was filtrated again with 3kDa Amicon Ultra centrifugal filters of 4 mL. The resultant filtrate was discarded, and the remaining volume was concentrated with 3kDa Amicon Ultra centrifugal filters of 500 µL. (Rodrigo et al., 2021)

Quality assessment was primarily achieved by resolving extracts in a discontinuous gel system, for one-dimensional separation of the extracted proteins under denaturing conditions by sodium dodecyl sulphate-polyacrylamide gel electrophoresis (SDS-PAGE) (Laemmli, 1970). Resolving and stacking gels contained 12% (v/v) and 6% (v/v) acrylamide, respectively. The running buffer consisted of 25 mM Tris, 192 mM glycine, and 3.5 mM SDS, and the molecular standard used was NZY Colour Protein Marker I (Nzytech), range 5-245 KDa. Gels were stained with Coomassie Blue overnight and transferred to a destaining solution the following day. Due to the low quantity of protein in the extracts, the gel was stained with Silver Nitrate following Coomassie Blue staining. For that, it was sensitized in 0.02% sodium thiosulfate solution for 1 minute. After washing with Milli-Q-grade ultrapure water ( $3 \times 20$  sec), the gel was incubated in 0,1% silver nitrate solution for 20 min. The gel was then washed with Milli-Q-grade ultrapure water ( $3 \times 20$  sec) and put into a new tray for development with a 3% sodium carbonate solution in the dark. To stop the developing process, it was washed in Milli-Q-grade ultrapure water for 20 sec and put in a 5% acetic acid solution. The gel was stored in a 1% acetic acid solution.

The extracts were then pooled into two samples: VM, and VE, containing the extract of red specimens and green specimens, respectively, and the buffer was exchanged for PBS using 3kDa Amicon Ultra centrifugal filters of 500  $\mu$ L. Protein was quantified using Bradford's method (Bradford, 1976), using bovine serum albumin (Sigma-Aldrich) as standard. Absorbance was read at 595 nm at room temperature in a Multiskan SkyHigh UV/Vis microplate spectrophotometer (Thermo Scientific).

Approximately three hours post fertilization, zebrafish embryos were dechorionated and exposed to different concentrations of two extract samples (VM- pooled exudate extracts from red specimens; VE- pooled exudate extracts from green specimens) for 72 hours in glass plates at 28°C. The exposure concentrations were 0 (control), 0.8, 0.6, 0.4, and 0.2  $\mu$ g/mL prepared in 5 mL of embryo medium and each was tested in 10 embryos, in triplicate. The development status of the embryos was observed and the live animals were counted once every 24 hours. At the end of 72 hours of exposure, the living specimens were fixed in paraformaldehyde (PFA) 4% and stored at 4°C Toxicity testing with zebrafish embryos wa done at *Instituto de Medicina Molecular Dr. João Lobo Antunes* (iMM).

## **2.4. Characterisation of the Venom Proteome**

Three red and three green sea anemones ( $n=3$ ) were retrieved from the rearing system and tentacles and oral disc were collected. The viscous liquid released in this process was added to the samples, avoiding carryover of debris. The tentacles were then excised and macerated with scissors and pestles. After that, samples were centrifuged for 15 min, 15000 rpm, at 4°C. The supernatant was transfered onto a fresh microtube and cold Milli-Q-grade ultrapure water was added to the pellet to repeat the process of

homogenization and centrifugation. The supernatants were centrifuged again for 15 min, 15000 rpm, at 4°C and protein concentration was determined using NanoDrop 2000 spectrophotometer (Thermo Fisher Scientific). For protein precipitation, acetone was added to the sample to a final concentration of 80%, and samples were kept, then, at -20°C until further use. The precipitate was centrifuged for 5 min, 5000 rpm, at 4°C, and the acetone supernatant was removed. Finally, samples underwent lyophilization in speed-vac, for 20 min, to eliminate traces of acetone (adapted from Macek & Lebez, 1988). The protein extract was resuspended in Tris-SDS buffer (0.5M Tris-HCl, pH 7.0; 10% SDS). The proteinaceous nature and quality of the extracts were assessed in a discontinuous gel system, as described above (Coomassie Blue staining only).

The protein extracts were pooled into two samples, red and green, and sent to Center for Neuroscience and Cell Biology (University of Coimbra) for LC-MS/MS analyses. There, extracts were run in a Short GelC approach. The gel was then stained with Coomassie Blue. Each lane of the gel was cut into 5 fractions and left overnight for destaining and porcine trypsin digestion. Then, the peptides were analyzed on a Eksigent NanoLC Ultra 2D separation system (Sciex) coupled to a TripleTOF 6600 mass spectrometer (Sciex). The chromatographic separation by micro-LC was achieved in a ChromXP C18CL column (0.3 × 150 mm, 3 μm, 120 Å, from Eksigent), at 50 °C. The flow rate was set to 5 μL/min, mobile phase A was 0.1% (v/v) formic acid plus 5% (v/v) DMSO in water and mobile phase B was 0.1% (v/v) formic acid plus 5% (v/v) DMSO in acetonitrile. The ESI DuoSpray™ ionization source was operated in the positive mode set to an ion spray voltage of 5500 V, 25 psi for nebulizer gas 1 (GS1) and the curtain gas (CUR). The rolling collision was used with a collision energy spread of 5. ProteinPilot 5.0.1 (Sciex) was used to execute peptide mass fingerprinting considering the parameters: cysteine alkylation by acrylamide, digestion by trypsin, and gel-based ID as a special factor. A customized database consisting of a subset of UniprotKB allocating toxin and venom-related proteins was used to annotate the resulting amino acid sequences through sequence homology using Blast (Altschul et al., 1990). The percentage of sequence coverage and number of matching peptides per protein established the accuracy of identification.

## 2.5. Statistical Analysis

Statistical analysis was executed with the software R 4.2.1 (Ihaka & Gentleman, 1996) and the level of significance ( $\alpha$ ) established for all analyses was 0.05.

The normality of data acquired from zebrafish embryo toxicity testing was assessed with the Shapiro-Wilk test, necessary for a parametric approach. Since the data did not follow a normal distribution ( $p$ -value < 0.05), the analysis proceeded with non-parametric tests, based on the Kruskal-Wallis H test, and

followed by Dunn's test for post-hoc comparisons. For a more detailed analysis, a new set of data was compiled to ignore the variable "Replica" and take into account the possibility of significant differences between times of observation. The same analysis was conducted on this set of data, as it showed not to follow a normal distribution (Appendix A.1). Additionally, correlation test using the Spearman method was conducted to assess the possibility of a dose-effect relationship for each time of observation (appendix A.2). Log-logistic response curves and EC50 values were estimated for the longest time of observation (72h) using a script previously developed in the host lab (BioModeller 1.01.05, with the required packages "MASS", "drc" and "tkrplot").

Gene Ontology (GO) analyses were performed on proteins annotated by contrasting against the customized toxin database mentioned above, using the package *UniprotR*. Through this, we retrieved the protein families corresponding to the Accession IDs of the identified proteins, along with the GO terms associated with Biological Process. This was executed for the Accession IDs of proteins exclusive to green specimens, exclusive to red specimens and common to both (Appendix A.3)



# 3.

## RESULTS

### 3.1. Histological analysis of *Actinia's* cnidocytes

The mouth of the polyp is centered in the oral disc and the tentacles arranged radially around the opening (Fig. 3.1A). The tentacles were shown to be relatively short, in a conical form, despite artefactual shrinking potentially caused by fixation (Fig.3.1B). The external structure of the polyp was observed as described in red and green specimens.

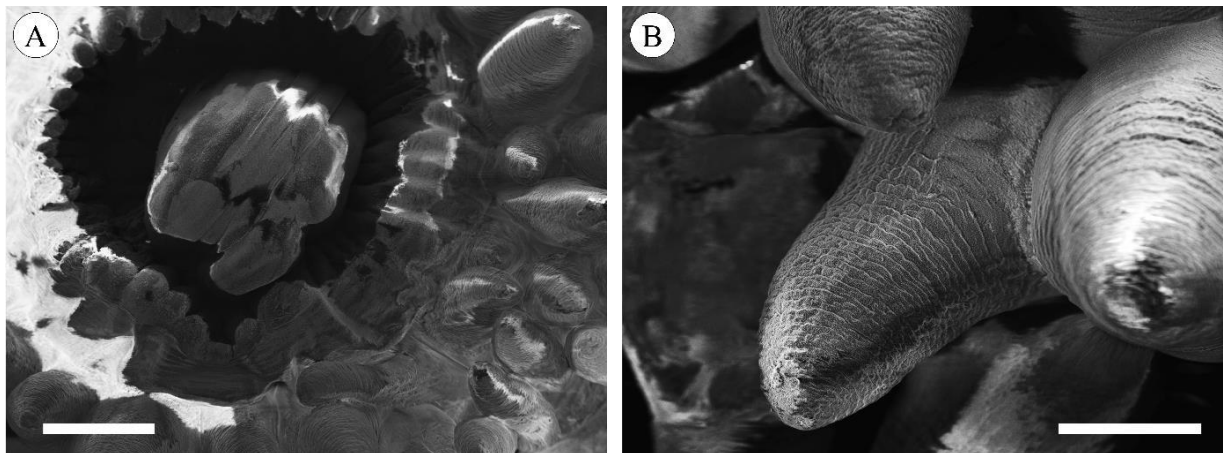


**Figure 3.1- External structure of *Actinia equina*.** (A) SEM image of the mouth of the polyp surrounded by radially arranged tentacles. (B) SEM image of a tentacle. Scale bars: (A) 1000 nm; (B) 600 nm.

As extensions of the body of the sea anemone, the gastrovascular cavity is also present within the tentacles (Fig. 3.2 B). The inner cellular layer, directly in contact with the cavity, was identified as the gastrodermis (endodermal origin), responsible for digestion and absorption of nutrients. The mesoglea, a cell-poor layer mostly comprised of connective tissue, separated the gastrodermis from the outer cellular layer, the epidermis (ectodermal origin), that lined the exterior of the polyp, tentacles included.

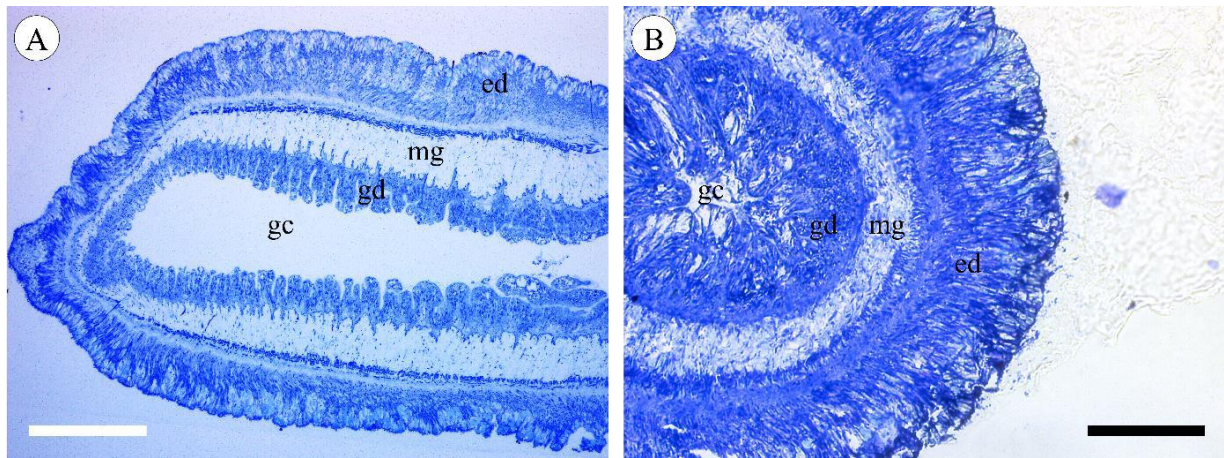


**Figure 3.2- Microanatomy of tentacles from green specimens of *Actinia equina*.** Longitudinal (A) and transversal (B) cross-sections of resin-embedded tentacles (Toluidine Blue stain), showing two cellular layers, the epidermis (ed) and gastrodermis (gd), separated by connective tissue, the mesoglea (mg). Scale bars: 200  $\mu$ m.

The epidermis (Fig.3.3) was composed of epithelial cells intercalated with mucocytes and anchored in a layer of fibrils. The base of the cells appeared thinner, where the nuclei are located, whereas the extremity of the cells was enlarged and sac-like, packed with vesicles (Fig. 3.3B), and the margin of the cells were covered in microvilli. It was also in this extremity that cnidocytes seem to be observed (Fig.3.3B), showing the nematocysts as an elongated body with a coiled thread appearance. These were distributed throughout the whole epidermis layer and more densely packed in the outer extremity of the layer. The microvilli in these cells are cnidocils, responsible for triggering the release of the nematocyst.

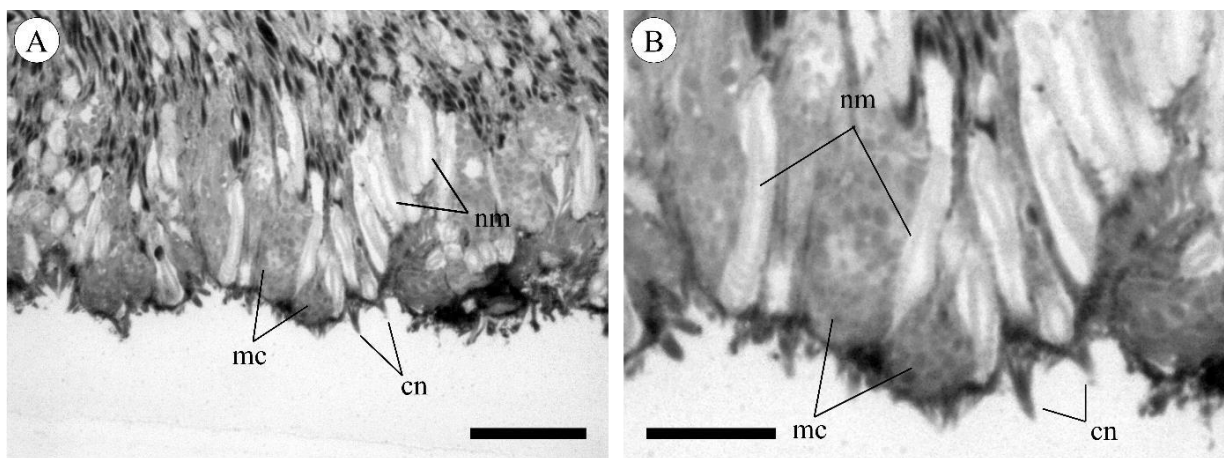


**Figure 3.3- The epidermis layer of a tentacle of a red specimen of *Actinia equina*** (A) Longitudinal cross-section of resin embedded tentacle (Toluidine Blue stain). (B) is a zoom-in on (A). cn- cnidocil; mc- mucocytes; nm- nematocysts. Scale bars: (A) 60  $\mu$ m; (B) 30  $\mu$ m

Histochemical staining of the epidermis of a tentacle showed that nematocysts had a distinct composition from the envolvent tissue. The epidermis revealed to be PAS-positive (pink), whereas the nematocysts were stained yellow (Picric Acid) (Fig.3.4 A). The nematocysts, along with some vesicles present in mucocytes, were densely stained with Coomassie Blue, indicating proteinaceous material. This was also

observed at the base of the epidermis cells, possibly indicating nematocyte precursor cells, the cnidoblasts.

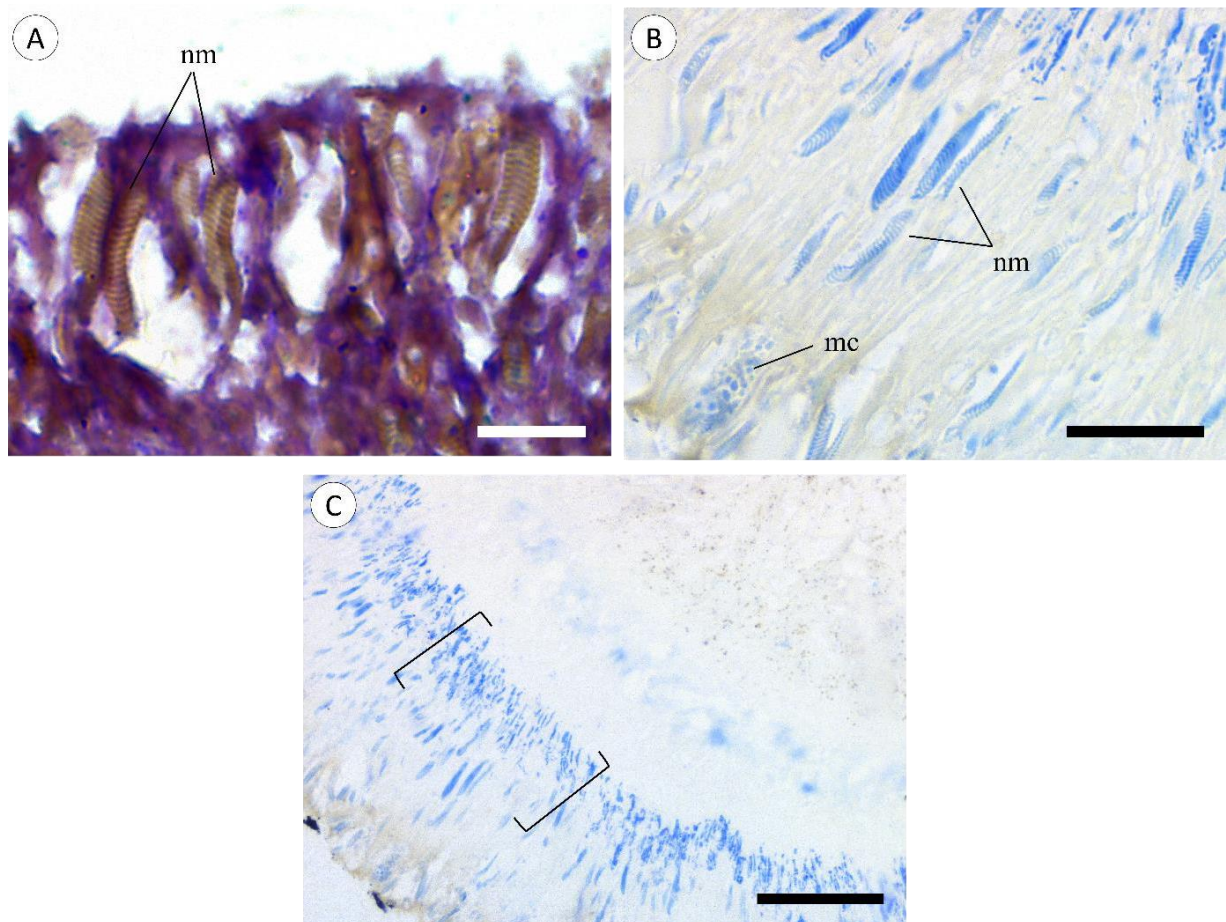


**Figure 3.4- Differentially stained cnidae in the epidermis of tentacles of an *A. equina*.** Transversal cross-sections of resin-embedded tentacles stained with (A) Tetrachromatic Stain and (B), (C) Coomassie Blue showing the presence of mucocytes (mc) and nematocysts (nm). (C) In brackets shows Coomassie Blue staining of a possible origin of the formation of nematocysts, the cnidoblasts. Scale bars: (A) 10  $\mu$ m, (B) 20  $\mu$ m, (C) 50  $\mu$ m

A closer look at the cnidae present in the epidermis of tentacles of green and red specimens (Fig. 3.5) confirmed the structure of the nematocysts, consisting of a hollow tube with an even diameter and spines throughout. It was possible to identify another class of cnidae, the spirocysts (Fig. 3.5 B) characterised by the small tubules arranged helically (as described in Shick, 1991).

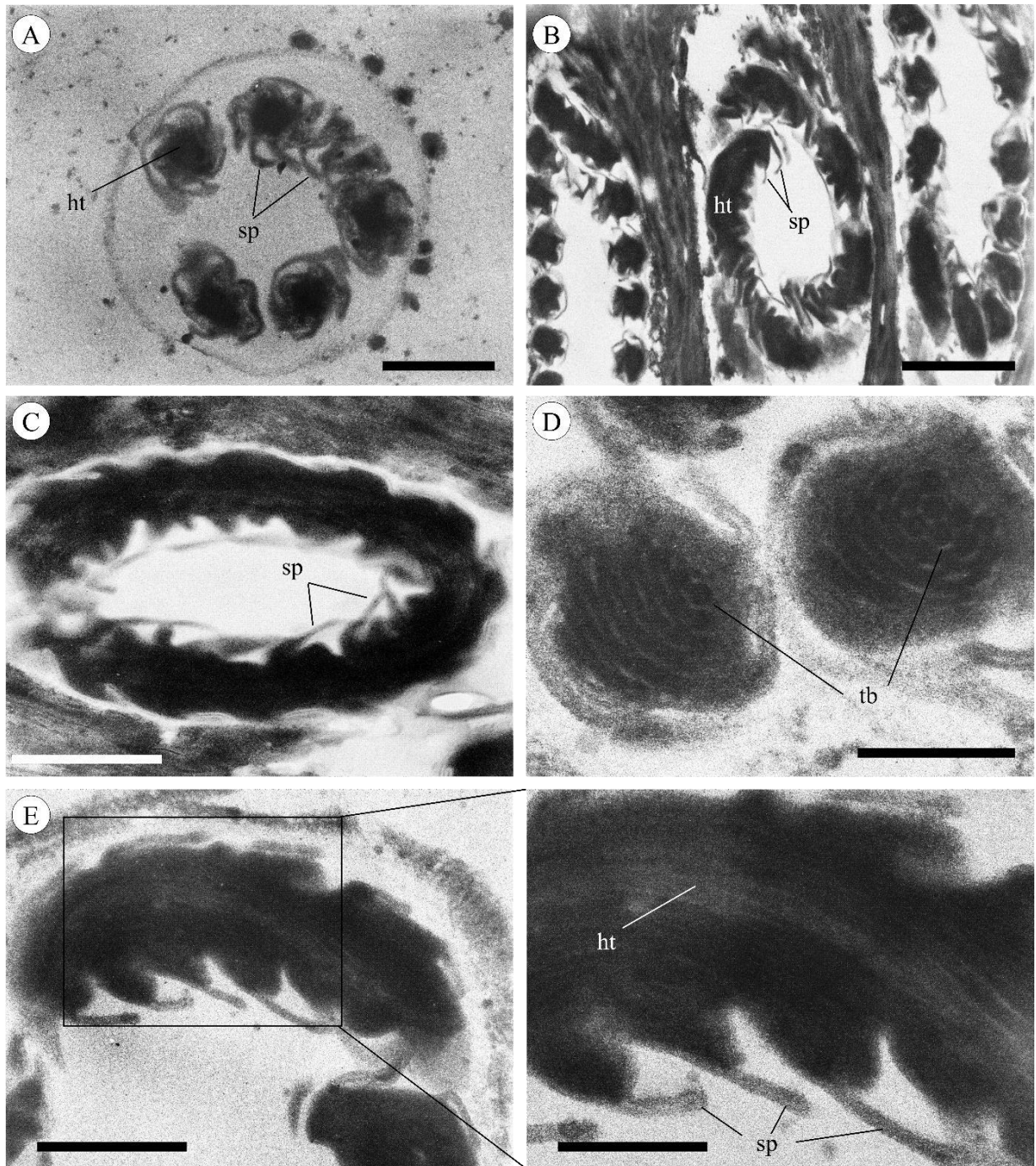


**Figure 3.5- Cnidae in the epidermis layer of tentacles of *Actinia equina*.** (A), (B) and (C) TEM images of cnidae in transversal cross-sections of resin-embedded tentacles of green specimens. (D) and (E) show TEM images of cnidae in transversal cross-sections of resin-embedded tentacles of red specimens. ht- hollow tube; sp- spines; tb- hollow tubules; Scale bars: (A) 800 nm, (B) 1200 nm, (C) 600 nm, (D) 200 nm; (E) 480 nm, inset: 240 nm.

Comparatively, the body wall of the sea anemones (Fig.3.6) was organized similarly to the tentacles, containing two cellular layers, the epidermis and gastrodermis, separated by the mesoglea. However, the epidermis of the column of the polyp did not display nematocysts and, although the majority of this layer was composed of mucocytes, these did not appear to contain as many vesicles as the ones identified in the epidermis of the tentacles (Fig. 3.3 B).

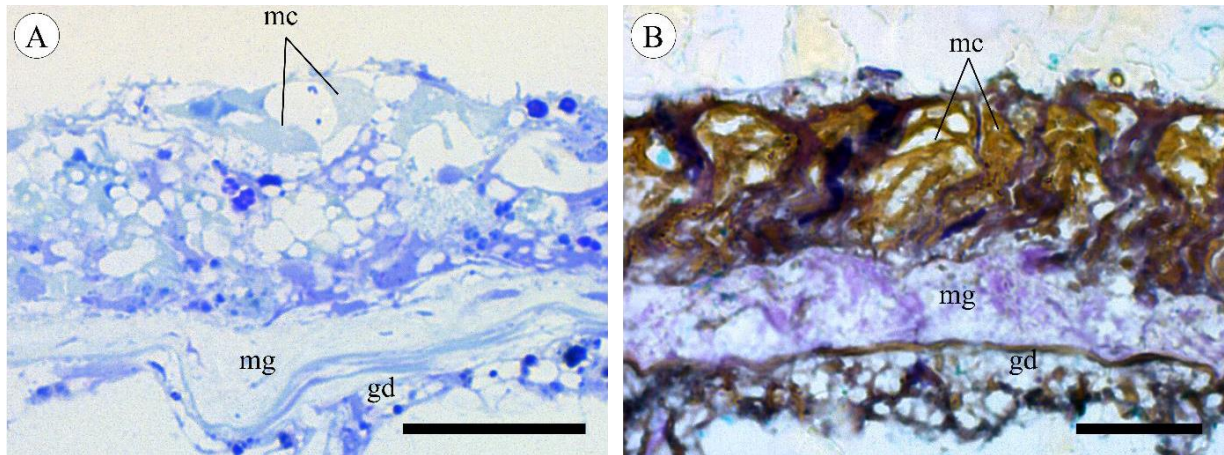


**Figure 3.6- Microanatomy of the body wall of *Actinia equina*.** (A) Transversal cross-section of a resin-embedded green specimen stained with Toluidine Blue. (B) Transversal cross-section of a resin-embedded red specimen stained with Tetrachromatic stain. gc- gastrodermis, mc- mucocytes, mg- mesoglea. Scale bars: (A), (B) 20 µm.

### 3.2. Toxicity Testing

Separation of the protein extracts (Fig. 3.7) showed major differences in band intensity between red and green specimens. Red specimen samples (N, O, and P samples in Fig.3.7) show some protein bands, with a varying pattern, that are not visible for green specimens (Q, R and S samples in Fig. 3.7). Overall, there are no signs of degradation of the samples, suggesting that the extracts from green specimens either lack proteinaceous content or the amount of protein loaded into the gel was insufficient to form visible bands.

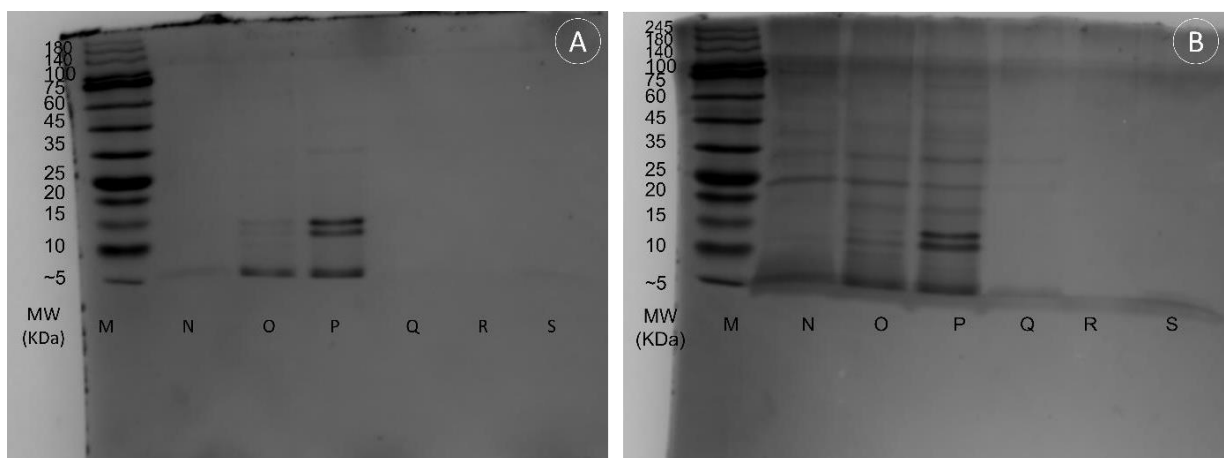
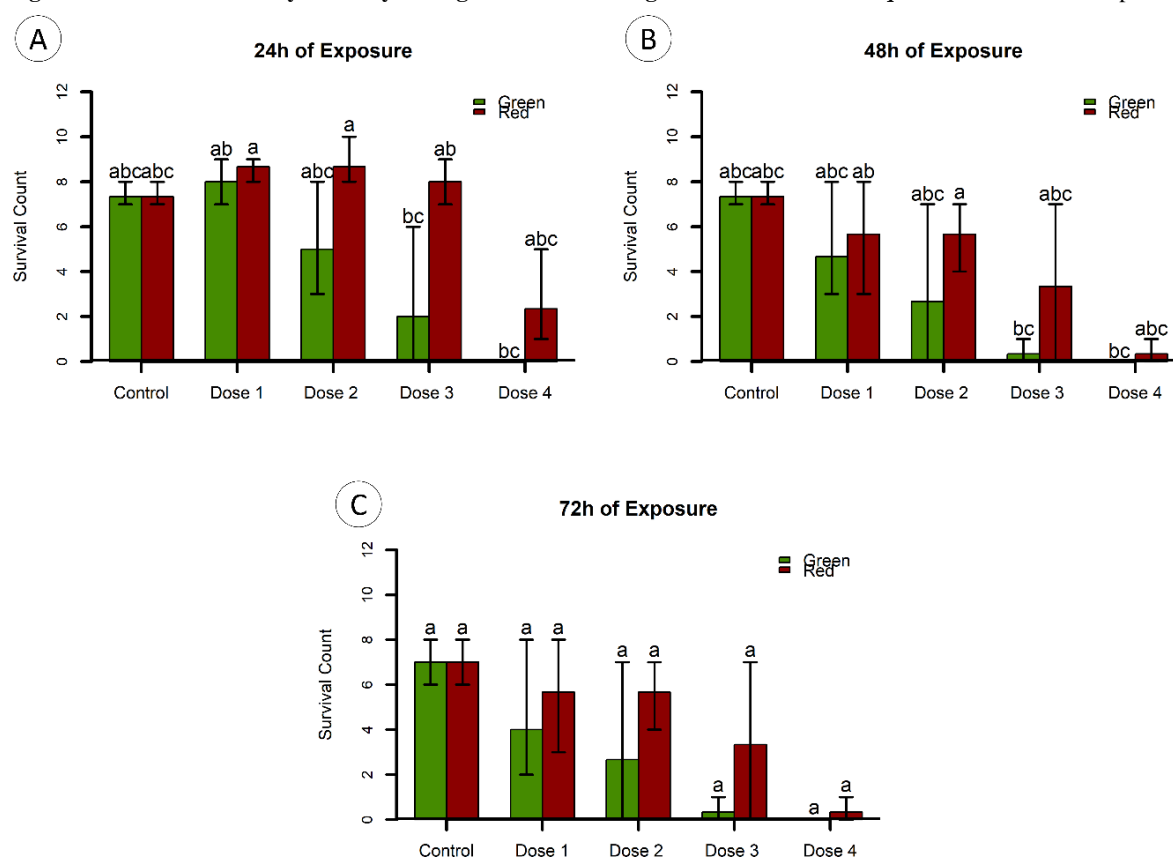


**Figure 3.7- SDS.PAGE of protein extracts of *Actinia equina* stained with Coomassie Blue (A) and Silver Nitrate (B).** Each well was loaded with the same quantity of total protein (5,85 µg). Samples N, O, and P belong to red specimens. Samples Q, R, and S belong to green specimens. The molecular standard used was NZY Colour Protein Marker I (Nzytech), range 5-245 KDa

The exposure of dechorionated zebrafish embryos to the pooled protein extracts showed that higher doses of protein (Doses 3 and 4, corresponding to 0.6 and 0.8 µg/mL of total protein, respectively) resulted in a significant decrease in survival of zebrafish embryos at 24 and 48 hours of exposure (Dunn's test;  $p < 0.05$ ). However, no significant differences were observed at 72 hours of exposure (Fig. 3.8). At 24h of exposure, significant differences were found for Dose 3 (0.6 µg/mL of total protein) of

both extracts, but only the green extract in the higher dose (0.8  $\mu\text{g}/\text{mL}$  of total protein) (Fig.3.8 A). As for 48h of exposure, significant differences were only found between lower doses of the red extract (Dose 1 and 2, corresponding to 0.2 and 0.4  $\mu\text{g}/\text{mL}$  of total protein, respectively) and the higher doses of the green extract (Dose 3 and 4) (Fig. 3.8 B).

**Figure 3.8- Zebrafish embryo toxicity testing of extracts from green and red *Actinia equina*** The results are expressed as



Survival Count + standard deviation, from zebrafish embryos exposed to different quantities of protein extracts from green and red specimens, plus control (zebrafish exposed to PBS) at (A) 24h, (B) 48h and (C) 72h of exposure. The letters (a, b and c) indicate significant differences between treatments (Dunn's test  $p < 0.05$ )

Additionally, when testing the effect of the variable “Color” against “Survival Count” for each time of observation ignoring all other variables, significant differences between green and red extracts were only found at 24h of exposure ( $p\text{-value} < 0.05$ ). Moreover, when assessing for a dose-effect relationship at each time of observation, a similar result was obtained, as a significant correlation was only found for green extracts at 24h of exposure, whereas for 48h and 72h of exposure it was found for both extracts. An estimated  $\text{EC}_{50}$  of 0.25 (0.08-0.77)  $\mu\text{g}/\text{mL}$  was obtained for green extracts (Fig. 3.9 A) and 0.61 (0.30-0.82)  $\mu\text{g}/\text{mL}$  for red extracts (Fig. 3.9 B).

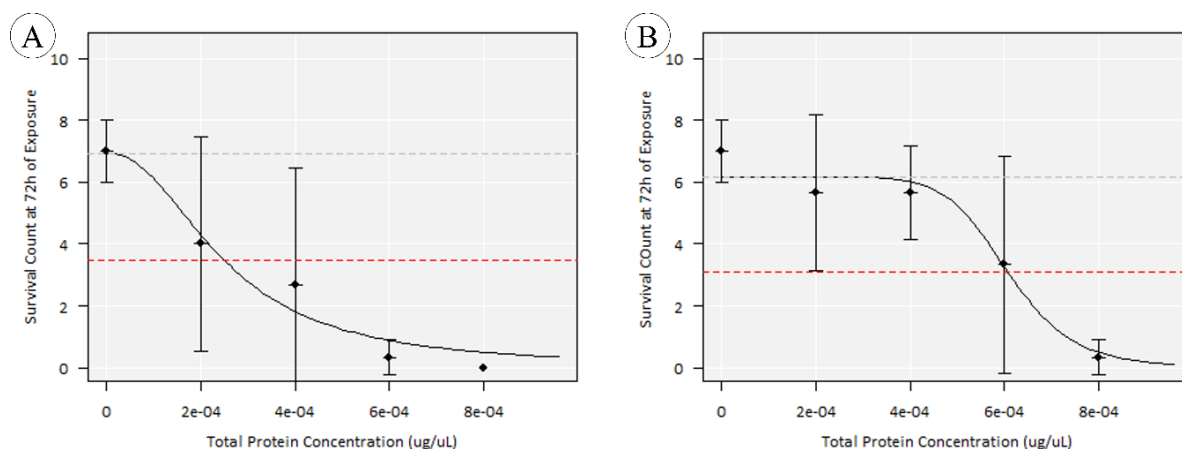


**Figure 3.9-** The effect of Total Protein Concentration ( $\mu\text{g}/\mu\text{L}$ ) over the Survival Count at 72h of Exposure for (A) green and (B) red extracts. EC50 corresponds to the intersection of the curve with the red line.

### 3.3. Characterisation of Venom Proteins

Separation of the protein extracts showed a successful extraction, with no signs of degradation and similar protein band patterns for all samples (Fig. 3.10). Additionally, samples from red specimen extracts (samples 1, 2 and 3 in Fig. 3.10) showed a more consistent profile of intensity than green specimen extracts (samples 4, 5 and 6 in Fig. 3.10). Moreover, the patterns of these samples differ from the ones obtained in the previous extraction (Fig.3.7), however, we cannot compare the intensity differences directly since the quantity of protein loaded into the gels between the two procedures was significantly different.

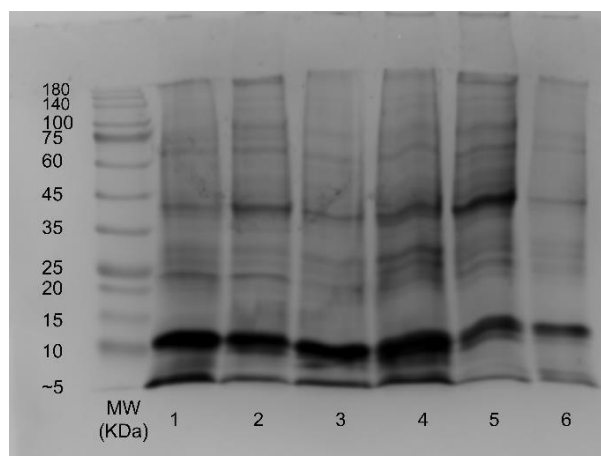


**Figure 3.10-** SDS-PAGE of protein extracts from *Actinia equina* stained with Coomassie Blue. Each well was loaded with the same quantity of total protein ( $11,5\mu\text{g}$ ). Samples 1, 2 and 3 belong to red specimens. Samples 4, 5 and 6 belong to green specimens. The molecular standard used was NZY Colour Protein Marker I (Nzytech), range 5-245 KDa.

The analysis of the pooled extracts by LC-MS/MS provided the identification of a total of 286 proteins. Of these, 68 were only identified in red specimen samples, 102 in green specimen samples, and 116 proteins were common to both proteins, of which 44, 55 and 56 were identified as toxins or toxin-like proteins, respectively. Examples of these are presented in Tables 3.1-3.3. It is important to note that

some of the toxins were specifically identified in *A.equina* itself, such as Delta-actitoxin-Aeq2a, common to both green and red specimen extracts, Delta-actitoxin-Aeq2b, exclusive to green specimen extract, and Delta-actitoxin-Aeq2b 2, exclusive to red specimen extract. The majority of the remaining toxins were identified in other cnidarians, such as *Actinia tenebrosa*, *Anemonia viridis* and *Anemonia sulcata*.

**Table 3.1- Examples of toxins commonly identified in green and red specimen extracts**, with the respective species, the number of peptides matched and the percentage of sequence coverage.

<b>Protein Name</b>	<b>Species</b>	<b>Number of Peptides</b>	<b>% Coverage</b>
Delta-actitoxin-Aeq2a	<i>Actinia equina</i>	11	100
PI-actitoxin-Aeq3c	<i>Actinia equina</i>	6	100
PI-actitoxin-Aeq3a	<i>Actinia equina</i>	5	100
U-actitoxin-Avd3n-like	<i>Actinia tenebrosa</i>	2	100
PI-actitoxin-Aeq3a-like	<i>Actinia tenebrosa</i>	4	100
U-actitoxin-Bgr3d	<i>Bunodosoma granuliferum</i>	1	100

**Table 3.2- Examples of toxins exclusively identified in green specimen extract**, with the respective species, the number of peptides matched and the percentage of sequence coverage.

<b>Protein Name</b>	<b>Species</b>	<b>Number of Peptides</b>	<b>% Coverage</b>
Delta-actitoxin-Aeq2b	<i>Actinia equina</i>	3	100
Delta-alicitoxin-Pse2a	<i>Phyllodiscus semoni</i>	1	100
Delta-alicitoxin-Pse2b	<i>Phyllodiscus semoni</i>	1	94.06
U-actitoxin-Avd9c	<i>Anemonia viridis</i>	1	100
Potassium channel toxin alpha-KTx 6.2	<i>Scorpius palmatus</i>	1	100
U16-lycotoxin-Ls1a	<i>Lycosa singoriensis</i>	1	100

**Table 3.3- Examples of toxins exclusively identified in red specimen extract** with the respective species, the number of peptides matched and the percentage of sequence coverage.

<b>Protein Name</b>	<b>Species</b>	<b>Number of Peptides</b>	<b>% Coverage</b>
U-actitoxin-Avd3s (Fragment)	<i>Anemonia viridis</i>	4	100
Delta-actitoxin-Aeq2b 2	<i>Actinia equina</i>	3	100
KappaPI-actitoxin-Ael3a	<i>Anthopleura elegantissima</i>	2	100
Type III potassium channel toxin protein	<i>Anemonia sulcata</i>	2	100
DELTA-thalatoxin-Avl2a	<i>Actinaria villosa</i>	2	100
Phospholipase A2 A2-actitoxin-Ucs2a	<i>Urticina crassicornis</i>	1	90.32

From the proteins identified exclusively in green and red specimens, the categories “Venom metalloproteinase (M12B)”, “Peptidase S1”, “Conotoxin O1” and “Arthropod phospholipase D” were common to both groups (Fig. 3.11). Proteins categorized as metalloproteinases were the most frequent in green specimen extracts, whereas the “venom Kunitz-Type family” was dominant in red specimen extract. Generally, proteins exclusive to green or red specimens were categorized as toxins, enzymes, or pathway inducing peptides.

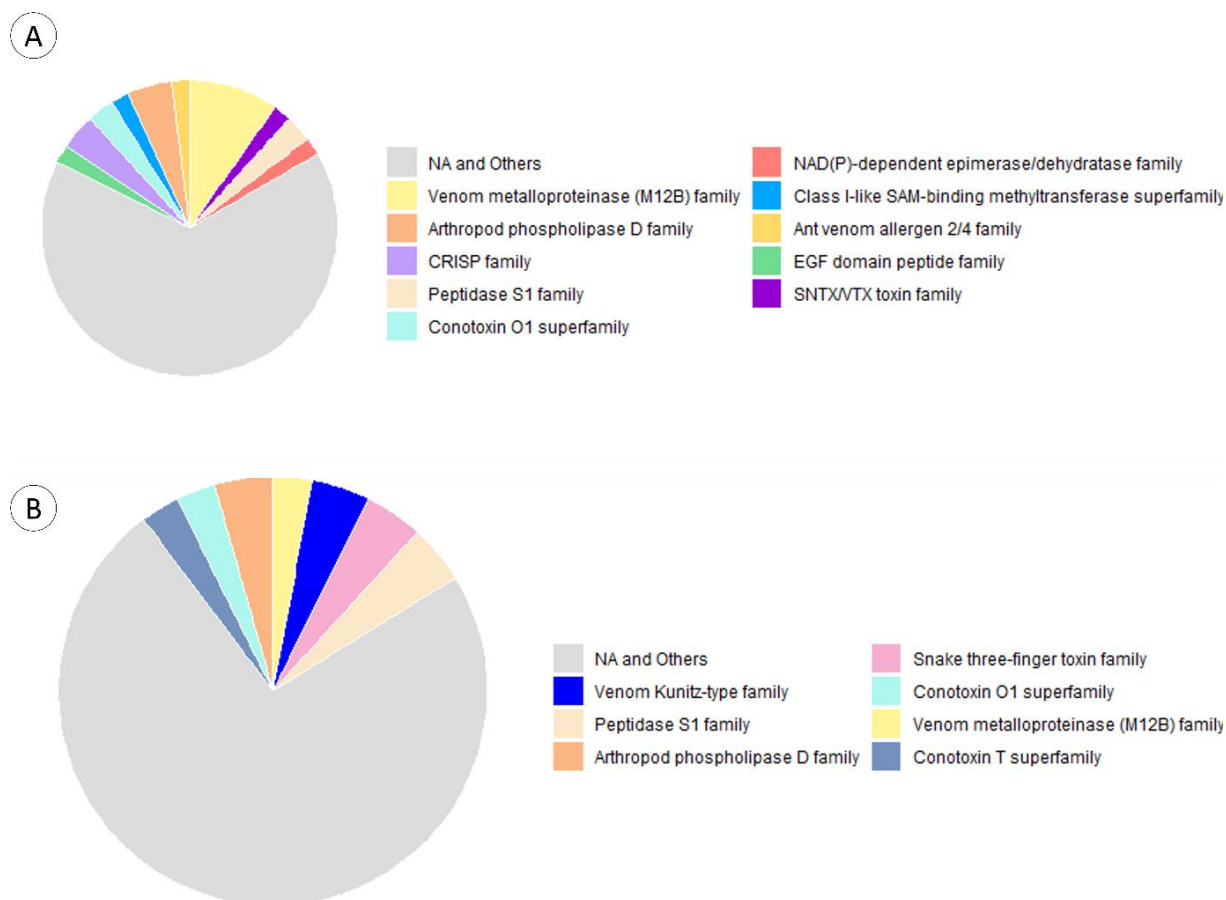


**Figure 3.11-** Pie charts illustrating the most abundant protein families identified in extracts from (A) green and (B) anemones.

The three most frequent ‘Biological Process’ GO terms in both red and green exclusive proteins were “proteolysis”, “hemolysis in another organism” and “lipid catabolic process” (Fig.3.12) and although bearing differences, the majority of terms across both groups refer to biological processes capable of inducing or potentiating toxicity. However, different proteins associated with the same GO term may not have the same effect, since it only indicates the process in which the proteins are involved and not the specific mode of action of each one.

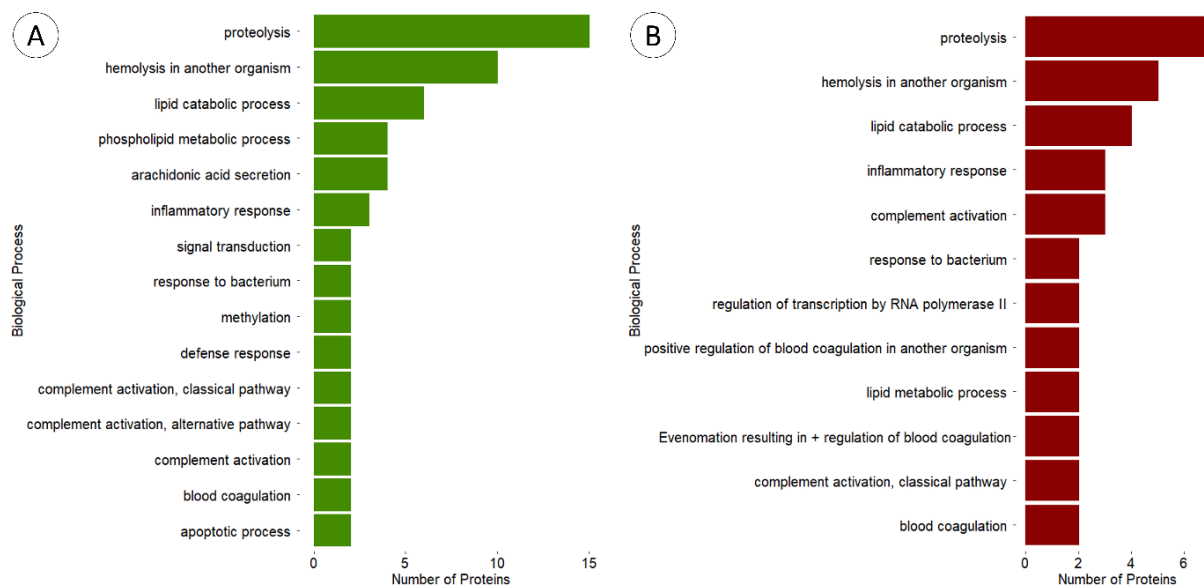


**Figure 3.12-** The number of proteins associated with the most frequent Biological Process Gene Ontology (GO) terms of proteins exclusively identified in extracts from (A) green and (B) red anemones.



## 4. DISCUSSION

This study demonstrated that *Actinia equina* has a well-differentiated venom system located in the tentacles, since there were no signs of venom-delivery structures in the body wall of the animals. Additionally, it has been demonstrated that the venom delivery system has no morphoanatomical differences between green and red varieties. This system seems to be responsible for the secretion of venom that contains proteinaceous toxins. Nonetheless, despite the conservations of the system, toxicity assays suggest that *Actinia* secrete toxins that can exert negative effects on the prey with differing efficacy depending on the variety, as the green specimen extracts showed a more potent, faster effect against zebrafish embryos, resulting in higher mortality. Foremost, the characterisation of the venom showed the presence of various proteins in the extracts, including toxins, with differences between green and red specimens, making the venom of *Actinia* an important research target for marine-derived drug discovery due to the potential of these compounds for biotechnological applications.

*Actinia equina*'s short and stout tentacles suggest that this species preys on macrofauna as an opportunistic suspension feeder (Ormond & Caldwell, 1982). The current study demonstrated that *A. equina* is armed with two cooperating types of cnidae in this action. The spirocysts, lacking spines, contain small helically arranged tubules that create an adhering surface upon release, gripping the prey without penetrating. These have been described to be the numerically dominant cnidae when observed and exclusive to the subclass Hexacorallia of the Phylum (Shick, 1991). Gripping to the prey may also be potentiated by the secretion of mucus, as cnidocytes were intercalated with mucocytes in tentacles. The nematocysts of *Actinia*, composed of a hollow tube bearing outward-directed spines, are then responsible for envenomation by injecting venom into the prey, as described for other cnidarians (Mariscal, 1984). Even though the body wall of *Actinia* is also lined with mucocytes, these are morphoanatomically different from mucocytes found in tentacles, which suggests that mucus secretion in the body wall is employed in protection. The venom system showed no variation between green and red specimens, but such resemblance is seemingly not extended to venom potency and composition, with the two subjects likely being interlinked. Indeed, toxicity assays revealed that venom extracts of *Actinia* have a toxicity effect on the survival of zebrafish embryos, despite the low concentration of the extracts, but green specimen extracts exerted a faster toxic effect, resulting in a lower EC50.

The complexity of venoms, as mixtures of various compounds, plus the variety of toxicological models, render comparisons difficult. Nonetheless, a similar study with crude venom extracted from the snake *Montivipera bornmuelleri* yielded an LD<sub>50</sub><sub>24h</sub> of 62 µg/mL of total protein in the venom extract (Sahyoun et al., 2022). Although the toxicity of the venom was tested in chorionated embryos, the referred study gives the understanding that the extracts obtained from *A. equina* are substantially toxic. Even though the extracts tended to cause a similar effect as the assay progressed (i.e., leading to full mortality of embryo batches), the initial discrepancy is indicative of distinct venom potency and, therefore, its composition between green and red specimens of *Actinia equina*. Characterising the venom proteome revealed important clues to explain the distinct potency of the extracts from the two varieties, even if, at the present stage, further studies on the specific modes of action are needed. The outcomes gave insight into this contrast, allowing the identification of interesting proteins and showing differences between red and green specimen extracts. Proteins with biotechnological potential were identified, toxins being the majority. Delta-actitoxin-Aeq2a, a toxin identified in both green and red specimen extracts, has been studied elsewhere. This protein, called Ae I, is a type I sodium channel inhibitory toxin that has been shown to have crab and mice toxicity (Lin et al. 1996). Similar toxins, with at least 50% similarity, were found exclusively in red or green specimen extracts, such as Delta-actitoxin-Aeq2b 2 and Delta-actitoxin-Aeq2b, respectively. Even though further research on the isolated toxins is necessary, it may be inferred that these toxins may have significantly contributed to the higher toxicity from green specimens, and implies that variance between *A. equina* varieties does exist. Additionally, Gene Ontology (GO) analysis revealed that both extracts have the same top three terms from 'Biological Process' search, but they are more frequent in the green specimen extract, which is congruent with the heightened toxicity from this extract. The majority of these terms referred to processes involved with toxicity, however, different proteins associated with the same process may not have the same mode of action, meaning that the actual role of the toxins in the observed toxicity would require further studies with the isolated toxins.

Noteworthy is the identification of proteins from other Cnidaria in the extracts of *Actinia*. Albeit expected, this not only sustains the toxicity and conserved status of toxins of these animals but also offers important validation of proteomics and its findings. In this case, for instance, AvTX-60A, a toxin from the sea anemone *Actinaria villosa* exclusively identified in red specimen extract (Oshiro et al., 2004), or PsTX-60A, a cytolytic toxin isolated from the nematocysts of *Phyllodiscus semoni*, exclusively identified in green specimen extract, that is believed to be one of the major causes of toxicity following stinging by this species which can be portrayed as dermatitis, local fever and ulceration in humans (Nagai et al., 2002). The aforementioned proteins belong to the same family, containing membrane-attack complex/perforin domains (MACPF), a common component of pore-forming proteins (Oshiro et al., 2004). Interestingly, pore-forming toxins (PFTs) are a well-studied group in *Actinia equina*. Actinoporins, namely Equinatoxin II, have been isolated from tentacles of *Actinia* and molecularly characterised (Ferlan & Lebez, 1974). These PFTs have been proposed as molecular probes, as well as immunotoxins, to identify and damage certain cancer cells containing different profiles of sphingomyelin in the membrane, since actinoporins have a high affinity to this sphingolipid (Ramirez-Carretero, 2020), making

the continuous research of *Actinia equina* even more relevant.

It must be noted that the extracts produced in the current study consisted of a mixture of proteins and not purified toxins, which by itself can imply that the quantities of each protein may fluctuate between extracts. Moreover, the extraction methods for toxicity assays and molecular characterisation of the venom were different, meaning that the resulting extracts were also distinct. Ultimately, the venom of *Actinia equina* is injected into the prey and not diffused, meaning that even though toxicity was tested on dechorionated zebrafish, the effects observed by exposure in the medium may be underestimated when compared to the natural venom injection by *Actinia*.



## 5. CONCLUSION

Marine bioactives present an important contribution to drug discovery, especially proteins, as these can provide safer, cost-effective and easily transformed compounds for biotechnological application and industrial scaled-up production. The characterisation of these marine products is crucial for the development of templates, allowing the synthetic reproduction of bioactivity while maintaining the marine habitats untouched. This work showed that cnidarians, even though relatively unexplored, can be an important source not only to provide a vast selection of bioactives but also specific toxins capable of interfering with biological processes involved in vital systems of the organism, thus representing the potential of the phylum for drug discovery.

This study revealed that *Actinia equina* possesses a well-differentiated venom system, implying the secretion of toxins directed to specific targets. Indeed, several proteins were identified, such as neurotoxins, that can affect specific systems of the prey. Additionally, the extracted proteins caused mortality of zebrafish embryos, validating the toxic nature of the venom of *Actinia equina*. One of the main findings of this work was the difference between red and green specimens, defined by the distinct toxicity efficacy of the extracts and the variance of protein identification between varieties. Furthermore, characterising the venoms allowed us to understand the interference of the proteins in biological processes targeted for toxicity, enhancing the potential biotechnological application of the species.

In future studies, the purification and fractioning of extracts would be of interest to explore the specific modes of action of the various components of the venoms, further contributing to explain the differential toxicity potency of the two varieties. In addition, it would be important to test the injection of the venom into model organisms to mimic the natural mechanism of envenomation by *Actinia equina*. Further studies of *Actinia equina* may contribute to blue biotechnology as a source of marine bioactives, such as actinoporins and other pore-forming proteins, which can be implemented in the development of anticancer drugs and other biomedical resources for human diseases.



## REFERENCES

- Altschul, S. F., et al., 1990. Basic local alignment search tool. *Journal of Molecular Biology* 215(3), 403-410 [https://doi.org/10.1016/S0022-2836\(05\)80360-2](https://doi.org/10.1016/S0022-2836(05)80360-2)
- Barcelos, M. C. S et al., 2018. The colors of biotechnology: General overview and developments of white, green and blue areas. *FEMS Microbiol. Lett.* **365**, 1–11 <https://doi.org/10.1093/femsle/fny239>
- Beeton, C. et al., 2005. Targeting effector memory T cells with a selective peptide inhibitor Kv1.3 channels for therapy of autoimmune diseases. *Molecular Pharmacology* 67(4), 1369-1381 <https://doi.org/10.1124/mol.104.008193>
- Bradford, M. M., 1976. A rapid and sensitive method for the quantification of microgram quantities of protein utilizing the principle of protein-dye binding. *Analytical Biochemistry* 72 (1-2), 248-254 [https://doi.org/10.1016/0003-2697\(76\)90527-3](https://doi.org/10.1016/0003-2697(76)90527-3)
- Burgess, J. G., 2012. New and emerging analytical techniques for marine biotechnology. *Curr. Opin. Biotechnol.* **23**, 29–33 <https://doi.org/10.1016/j.copbio.2011.12.007>
- Calvete, J. J. et al., 2009. Venoms, venomics, antivenomics. *FEBS Letters* **583**, 1736-1743 <https://doi.org/10.1016/j.febslet.2009.03.029>
- Christinat, A. & Leyvraz, S., 2009. Role of trabectedin in the treatment of soft tissue sarcoma. *Onco. Targets. Ther.* **2**, 105–113 <https://doi.org/10.2147/ott.s4454>
- Costa, P.M., 2018 *The Handbook of Histopathological Practices in Aquatic Environments*; Academic Press: Cambridge, MA, USA; ISBN 9780128120323.
- D’Ambra, I. & Lauritano, C., 2020. A Review of toxins from cnidaria. *Mar. Drugs* **18**, 1–28 <https://doi.org/10.3390/md18100507>
- Ferlan, I. & Lebez, I., 1974. Equinatoxin, a lethal protein from *Actinia equina*- I Purification and characterization. *Toxicon* 12(1), 57-58 [https://doi.org/10.1016/0041-0101\(74\)90099-3](https://doi.org/10.1016/0041-0101(74)90099-3)
- Fish, J. D. & Fish, S., 2011. A student’s guide to the seashore. *Cambridge University Press* 86-125
- Frazão, B. et al. 2012. Sea Anemone (Cnidaria, Anthozoa, Actiniaria) Toxins: An Overview. *Mar. Drugs*, **10**, 1812-1851 <https://doi.org/10.3390/md10081812>
- Inoué, T. & Osatake, H., 1988. A new drying method of biological specimens for scanning electron microscopy: the t-butyl alcohol freeze-drying method. *Arch Histol Cytol* 51(1), 53-59 <https://doi.org/10.1679/aohc.51.53>
- Jouiaei, M. et al., 2015. Ancient Venom Systems: A Review on Cnidaria Toxins. *Toxins* **7**, 2251-2271 <https://doi.org/10.3390/toxins7062251>
- Kong, D. et al., 2010. Marine natural products as sources of novel scaffolds: achievement and concern. *Drug Discovery Today* **15**(21-22), 884-886. <https://doi.org/10.1016/j.drudis.2010.09.002>
- Laemmli, U.K., 1970. Cleavage of structural proteins during the assembly of the head of bacteriophage T4. *Nature*. 227, 680-685. <https://doi.org/10.1038/227680a0>
- Lin, X. et al., 1996. A polypeptide toxin in the sea anemone *Actinia equina* homologous with other sea anemone sodium channel toxins: Isolation and amino acid sequence. *Toxicon* 34(1), 57-65 [https://doi.org/10.1016/0041-0101\(95\)00121-2](https://doi.org/10.1016/0041-0101(95)00121-2)
- Lindequist, U., 2016. Marine-Derived Pharmaceuticals – Challenges and Opportunities. *Biomol Ther* **24**, 561-571 <https://doi.org/10.4062/biomolther.2016.181>

- Macek, P. & Lebez, D., 1988. Isolation and Characterization of Three Lethal and Hemolytic Toxins from the Sea Anemone *Actinia equina* L. *Toxicon* 26(5), 441-451 [https://doi.org/10.1016/00410101\(88\)90183-3](https://doi.org/10.1016/00410101(88)90183-3)
- Mariscal, R.N., 1984. Cnidaria: Cnidae. *Biology of the Integument*, 57-68 [https://doi.org/10.1007/978-3-642-51593-4\\_6](https://doi.org/10.1007/978-3-642-51593-4_6)
- Menezes, C. & Thakur, N. L., 2022. Sea anemone venom: Ecological interactions and bioactive potential. *Toxicon* 208, 31-46 <https://doi.org/10.1016/j.toxicon.2022.01.004>
- Montaser, R., & Luesch, H. 2011. Marine natural products: a new wave of drugs?. *Future medicinal chemistry*, 3(12), 1475–1489. <https://doi.org/10.4155/fmc.11.118>
- Molinski, T. F. et al., 2009. Drug development from marine natural products. *Nat. Rev. Drug Discov.* **8**, 69–85 <https://doi.org/10.1038/nrd2487>
- Nagai, H., et al., 2002. Novel proteinaceous toxins from the nematocyst venom of the Okinawan sea anemone *Phyllo-discus semoni* Kwietniewski. *Biochemical and biophysical research communications*, 294(4), 760–763. [https://doi.org/10.1016/S0006-291X\(02\)00547-8](https://doi.org/10.1016/S0006-291X(02)00547-8)
- Ormond, G.F.R., Caldwell, S., 1982. The effect of oil pollution on the reproduction and feeding behaviour of the sea anemone *Actinia equina*. *Marine Pollution Bulletin* 13(4), 118 – 122 [https://doi.org/10.1016/0025-326X\(82\)90367-8](https://doi.org/10.1016/0025-326X(82)90367-8)
- Oshiro, N., et al., 2004. A new membrane-attack complex/perforin (MACPF) domain lethal toxin from the nematocyst venom of the Okinawan sea anemone *Actinaria villosa*. *Toxicon* ,43(2), 225–228. <https://doi.org/10.1016/j.toxicon.2003.11.017>
- Ramírez-Carretero S., et al., 2020. Actinoporins: From the Structure and Function to the Generation of Biotechnological and Therapeutic Tools. *Biomolecules*, 10(4):539. <https://doi.org/10.3390/biom10040539>
- Rocha, J. et al., 2011. Cnidarians as a source of new marine bioactive compounds - An overview of the last decade and future steps for bioprospecting. *Mar. Drugs* **9**, 1860–1886 <https://doi.org/10.3390/md9101860>
- Rodrigo, A.P. et al., 2022. Endogenous Fluorescent Proteins in the Mucus of an Intertidal Polychaeta: Clues fro Biotechnology. *Mar. Drugs* 20(4), 224 <https://doi.org/10.3390/md20040224>
- Sahyoun, C et al, 2022 Neuro- and Cardiovascular Activities of *Montivipera bornmuelleri* Snake Venom. *Biology* 11, 888. <https://doi.org/10.3390/biology11060888>
- Sher, D. et al. 2005. Hydralisinins, a New Category of  $\beta$ -Pore-forming Toxins in Cnidaria. *J Biol Chem.*, 280(24), 22847–22855 <https://doi.org/10.1074/jbc.M503242200>
- Shick, J. M., 1991. Overview of sea anemones. *A Functional Biology of Sea Anemones* 1-35 [https://doi.org/10.1007/978-94-011-3080-6\\_1](https://doi.org/10.1007/978-94-011-3080-6_1)
- Tarcha, E. J. et al., 2017. Safety and pharmacodynamics of dalazatide, a Kv1.3 channel inhibitor, in the treatment of plaque psoriasis: A randomized phase 1b trial. *PloS ONE* 12(7), e0180762 <https://doi.org/10.1371/journal.pone.0180762>
- Turk, T. & Kem, W. R., 2009. The phylum Cnidaria and investigations of its toxins and venoms until 1990. *Toxicon*, 54 (8), 1031-1037 <https://doi:10.1016/j.toxicon.2009.06.031>
- Upadhyay, S. K. et al., 2013. Selective Kv1.3 channel blocker as therapeutic for obesity and insulin resistance. *Proceedings of the National Academy of Sciences of the United States of America*, 110(24), E2239–E2248 <https://doi.org/10.1073/pnas.1221206110>
- Venable, J.H., Coggeshall, R., 1965. A simplified lead citrate stain for use in electron microscopy. *Journal of Cell Biology* 25, 407-413 <https://doi.org/10.1083/jcb.25.2.407>
- Williams, J. A. et al., 2008. Ziconotide: An update and review. *Expert Opin. Pharmacother.* **9**, 1575–1583 <https://doi.org/10.1517/14656566.9.9.1575>

## APPENDICES

### Appendix 1- R script for the statistical analysis of zebrafish embryo toxicity testing data.

```
##The p-value was set to 0.05 for all analyses
```

```
##Import Data
```

```
fileName<-"ZF_Results.csv"
```

```
ZebrafishTable<-read.table(fileName, header=TRUE, row.names=1, sep=";", dec=",")
```

```
ZebrafishTable$Treatment<-as.factor(ZebrafishTable$Treatment)
```

```
ZebrafishTable$Color<-as.factor(ZebrafishTable$Color)
```

```
##Shapiro Wilk's test for normality check
```

```
for(i in 4:ncol(ZebrafishTable))
```

```
{
```

```
  print(paste(sep=" ", "Variable= ", colnames(ZebrafishTable)[i]))
```

```
  print(shapiro.test(ZebrafishTable[,i]))
```

```
  windows()
```

```
  qqnorm(ZebrafishTable[,i])
```

```
}
```

```
##Kruskal Wallis test
```

```
kruskal24hReplica<-kruskal.test(data=ZebrafishTable, Alive24h~Replicate)
```

```
kruskal48hReplica<-kruskal.test(data=ZebrafishTable, Alive48h~Replicate)
```

```
kruskal72hReplica<-kruskal.test(data=ZebrafishTable, Alive72h~Replicate)
```

```
kruskal24hColor<-kruskal.test(data=ZebrafishTable, Alive24h~Color)
```

```
kruskal48hColor<-kruskal.test(data=ZebrafishTable, Alive48h~Color)
```

```
kruskal72hColor<-kruskal.test(data=ZebrafishTable, Alive72h~Color)
```

```
kruskal24hTreatment<-kruskal.test(data=ZebrafishTable, Alive24h~Treatment)
```

```
kruskal48hTreatment<-kruskal.test(data=ZebrafishTable, Alive48h~Treatment)
```

```
kruskal72hTreatment<-kruskal.test(data=ZebrafishTable, Alive72h~Treatment)
```

```

##Import new data set
fileName<-"ZF_Results_all_comp.csv"
DataZF<-read.table(fileName, header=TRUE, row.names=1, sep=";", dec=",")

DataZF$Treatment<-as.factor(DataZF$Treatment)
treatments<-levels(DataZF$Treatment)

##Shapiro Wilk's test for normality check
for(i in 2:ncol(DataZF))
{
  print(paste(sep=" ", "Variable= ", colnames(DataZF)[i]))
  print(shapiro.test(DataZF[,i]))
  windows()
  qqnorm(DataZF[,i])
}

##Kruskal Wallis test
kruskaltest<-kruskal.test(data=DataZF, Alive~Treatment)

##Dunn's test
##Loading required packages
library(dunn.test)

DunnTestTotal<-dunn.test(DataZF$Alive, g=DataZF$Treatment, altp=FALSE, method="bh")
dunnT<-as.data.frame(cbind(DunnTestTotal$comparisons, DunnTestTotal$altP.adjusted))
dunnT<-as.matrix(DunnTestTotal$P.adjusted)
rownames(dunnT)<-gsub(" ", "", DunnTestTotal$comparisons)

```

## Appendix 2- R script for correlation testing of zebrafish embryo toxicity testing data, using the Spearman method.

### ##Import Data

```
fileName<-"cor.test_Data.csv"
```

```
corData<-read.table(fileName, header=TRUE, row.names=1, sep=";", dec=",")
```

### ##Subsetting the red and green specimen extract data for each time of observation

```
green<-subset(corData, corData[,2]=="G")
```

```
greenMeans24h<-aggregate(data=green, Alive24h~Treatment, mean, na.rm=TRUE)
```

```
greenMeans48h<-aggregate(data=green, Alive48h~Treatment, mean, na.rm=TRUE)
```

```
greenMeans72h<-aggregate(data=green, Alive72h~Treatment, mean, na.rm=TRUE)
```

```
red<-subset(corData, corData[,2]=="R")
```

```
redMeans24h<-aggregate(data=red, Alive24h~Treatment, mean, na.rm=TRUE)
```

```
redMeans48h<-aggregate(data=red, Alive48h~Treatment, mean, na.rm=TRUE)
```

```
redMeans72h<-aggregate(data=red, Alive72h~Treatment, mean, na.rm=TRUE)
```

### ##Correlation Test with Spearman method

```
corGreen24h<-cor.test(greenMeans24h[,1], greenMeans24h[,2], method="spearman", exact=FALSE)
```

```
corRed24h<-cor.test(redMeans24h[,1],redMeans24h[,2], method="spearman", exact = FALSE)
```

```
corGreen48h<-cor.test(greenMeans48h[,1], greenMeans48h[,2], method="spearman", exact=FALSE)
```

```
corRed48h<-cor.test(redMeans48h[,1],redMeans48h[,2], method="spearman", exact = FALSE)
```

```
corGreen72h<-cor.test(greenMeans72h[,1], greenMeans72h[,2], method="spearman", exact=FALSE)
```

```
corRed72h<-cor.test(redMeans72h[,1],redMeans72h[,2], method="spearman", exact = FALSE)
```

### Appendix 3- R script for Gene Ontology (GO) analysis of LC-MS/MS data

#### ##Import Data

```
fileName1<-"Proteins_Green_ProteinHits.csv"  
Green_ProteinHits<-read.table(fileName1, header=TRUE, row.names=1, sep=";", dec=".", quote="")
```

```
fileName2<-"Proteins_Red_ProteinHits.csv"
```

```
Red_ProteinHits<-read.table(fileName2, header=TRUE, row.names=1, sep=";", dec=".", quote = "")
```

#### ##Determine exclusive Accession ID's in red and green extracts and common to both extracts.

```
EqualHits<-as.vector(intersect(Green_ProteinHits$Accession, Red_ProteinHits$Accession))
```

```
CommonHits<-Green_ProteinHits[Green_ProteinHits$Accession %in% EqualHits,]
```

```
DifferentGreen<-as.vector(setdiff(Green_ProteinHits$Accession, Red_ProteinHits$Accession))
```

```
DiffHitsGreen<-Green_ProteinHits[Green_ProteinHits$Accession %in% DifferentGreen,]
```

```
nrow(DiffHitsGreen)
```

```
DifferentRed<-as.vector(setdiff(Red_ProteinHits$Accession, Green_ProteinHits$Accession))
```

```
DiffHitsRed<-Red_ProteinHits[Red_ProteinHits$Accession %in% DifferentRed,]
```

```
nrow(DiffHitsRed)
```

#### ##Download of GO terms associated with Accession ID's from green or red specimen extracts data

#### ##Loading required packages

```
library(httr)
```

#### ##Download

```
UniprotDownload<-function (ProteinAccList, Colnames)
```

```
{
```

```
  message("Please wait we are processing your accessions ...")
```

```
  pb <- progress::progress_bar$new(total = length(ProteinAccList))
```

```
  baseUrl <- "http://uniprot.org/uniprotkb/search?"
```

```
  ProteinInfoParsed_total = data.frame()
```

```
  for (ProteinAcc in ProteinAccList) {
```

```
    Request <- tryCatch({
```

```
      GET(paste0(baseUrl, "?query=accession:", ProteinAcc), timeout(7))
```

```
    }, error = function(cond) {
```

```
      message("Internet connection problem occurs and the function will return the original error")
```

```
      message(cond)
```

```

})
ProteinName_url <- paste0("?query=accession:", ProteinAcc,
                           "&format=tsv&fields=", Colnames)
RequestUrl <- paste0(baseUrl, ProteinName_url)
RequestUrl <- URLEncode(RequestUrl)
if (length(Request) == 0) {
  message("Internet connection problem occurs")
  return()
}
if (Request$status_code == 200) {
  ProteinDataTable <- tryCatch(read.csv(RequestUrl,
                                       header = TRUE, sep = "\t"), error = function(e) NULL)
  if (!is.null(ProteinDataTable)) {
    ProteinDataTable <- ProteinDataTable[1, ]
    ProteinInfoParsed <- as.data.frame(ProteinDataTable,
                                       row.names = ProteinAcc)
    ProteinInfoParsed_total <- rbind(ProteinInfoParsed_total,
                                     ProteinInfoParsed)
  }
}
else {
  HandleBadRequests(Request$status_code)
}
pb$tick()
}
return(ProteinInfoParsed_total)
}

Green_ProteinHits$AccessionID<-unlist(sapply(Green_ProteinHits$Accession,      function(x)  un-
list(strsplit(x, "|", fixed = TRUE))[2]))
Red_ProteinHits$AccessionID<-unlist(sapply(Red_ProteinHits$Accession,        function(x)  un-
list(strsplit(x, "|", fixed = TRUE))[2]))

Green_ProteinHits[,c(12:15)]<-UniprotDownload(Green_ProteinHits$AccessionID,   "protein_fami-
lies,go_p,go_f,go_c")
Red_ProteinHits[,c(12:15)]<-UniprotDownload(Red_ProteinHits$AccessionID,     "protein_fami-
lies,go_p,go_f,go_c")

```

### ##Subsetting data exclusive to green or red specimen extracts

```
DifferencesRed<-subset(Red_ProteinHits, Red_ProteinHits$Accession %in% DifferentRed)
nrow(DifferencesRed)
DifferencesGreen<-subset(Green_ProteinHits, Green_ProteinHits$Accession %in% DifferentGreen)
nrow(DifferencesGreen)
```

### ##Subsetting data for the most abundant protein families chart

```
UniqueFamilyRed<-(unique(DifferencesRed[,12]))
length(UniqueFamilyRed)
UniqueFamilyRed<-unlist(sapply(UniqueFamilyRed, function(x) unlist(strsplit(x, ",", fixed =
TRUE))[1]))
UniqueFamilyRed<-as.data.frame(unique(UniqueFamilyRed))
UniqueFamilyRed$NumberORFs<-sapply(UniqueFamilyRed[,1], function(x) length(which(grepl(x,
DifferencesRed[,12], fixed = TRUE))))
UniqueFamilyRed$NumberORFs[which(is.na(UniqueFamilyRed[,1]))]<-length(which(is.na(Differ-
encesRed[,12])))
UniqueFamilyRed<-UniqueFamilyRed[order(-UniqueFamilyRed$NumberORFs),]
rownames(UniqueFamilyRed)<-NULL
sum(UniqueFamilyRed$NumberORFs)
GraphRed<-UniqueFamilyRed[1:8,]
GraphRed[1,2]<-GraphRed[1,2]+sum(UniqueFamilyRed[,2])-sum(GraphRed[,2])
sum(GraphRed$NumberORFs)

UniqueFamilyGreen<-(unique(DifferencesGreen[,12]))
length(UniqueFamilyGreen)
UniqueFamilyGreen<-unlist(sapply(UniqueFamilyGreen, function(x) unlist(strsplit(x, ",", fixed =
TRUE))[1]))
UniqueFamilyGreen<-as.data.frame(unique(UniqueFamilyGreen))
UniqueFamilyGreen$NumberORFs<-sapply(UniqueFamilyGreen[,1], function(x)
length(which(grepl(x, DifferencesGreen[,12], fixed = TRUE))))
UniqueFamilyGreen$NumberORFs[which(is.na(UniqueFamilyGreen[,1]))]<-length(which(is.na(Dif-
ferencesGreen[,12])))
UniqueFamilyGreen<-UniqueFamilyGreen[order(-UniqueFamilyGreen$NumberORFs),]
rownames(UniqueFamilyGreen)<-NULL
sum(UniqueFamilyGreen$NumberORFs)
GraphGreen<-UniqueFamilyGreen[1:11,]
GraphGreen[1,2]<-GraphGreen[1,2]+sum(UniqueFamilyGreen[,2])-sum(GraphGreen[,2])
```

```
sum(GraphGreen$NumberORFs)
```

```
##Subsetting data for most frequent 'Biological Process'GO terms from proteins exclusive to green and red specimen extracts
```

```
Terms<-c()
NACount<-0
for(i in 1:nrow(DifferencesRed)){
  GOAux<-sapply(DifferencesRed[i,13], function(x) unlist(strsplit(x,"; ", fixed=TRUE)))
  if(!is.na(GOAux[1]))
    Terms<-rbind(Terms, GOAux)
  else
    NACount<-NACount+1
}
```

```
UniqueProcessRed<-as.data.frame(unique(Terms[,1]))
colnames(UniqueProcessRed)[1]<-"Process"
UniqueProcessRed$Process<-unlist(sapply(UniqueProcessRed$Process, function(x) unlist(strsplit(x,
"[" , fixed = TRUE))[1])))
```

```
UniqueProcessRed$NumberORFs<-sapply(UniqueProcessRed[,1], function(x) length(which(grepl(x,
DifferencesRed[,13], fixed = TRUE))))
UniqueProcessRed$NumberORFs[which(is.na(UniqueProcessRed[,1]))]<-length(which(is.na(DifferencesRed[,13])))
UniqueProcessRed<-UniqueProcessRed[order(-UniqueProcessRed$NumberORFs),]
rownames(UniqueProcessRed)<-NULL
```

```
Terms<-c()
NACount<-0
for(i in 1:nrow(DifferencesGreen)){
  GOAux<-sapply(DifferencesGreen[i,13], function(x) unlist(strsplit(x,"; ", fixed=TRUE)))
  if(!is.na(GOAux[1]))
    Terms<-rbind(Terms, GOAux)
  else
    NACount<-NACount+1
}
```

```

UniqueProcessGreen<-as.data.frame(unique(Terms[,1]))
colnames(UniqueProcessGreen)[1]<-"Process"
UniqueProcessGreen$Process<-unlist(sapply(UniqueProcessGreen$Process,      function(x)      un-
list(strsplit(x, "[", fixed = TRUE))[1]))
UniqueProcessGreen$NumberORFs<-sapply(UniqueProcessGreen[,1],      function(x)
length(which(grepl(x, DifferencesGreen[,13], fixed = TRUE))))
UniqueProcessGreen$NumberORFs[which(is.na(UniqueProcessGreen[,1]))]<-length(which(is.na(Dif-
ferencesGreen[,13])))
UniqueProcessGreen<-UniqueProcessGreen[order(-UniqueProcessGreen$NumberORFs),]
rownames(UniqueProcessGreen)<-NULL

```





2022

MARIA ALCAIDE

DRUG DISCOVERY FROM CNIDARIANS: DELIVERY, BIOREACTIVITY AND

